Research Article

David J. Unger*

Antiplane point load solution for a linear slot with rounded ends

https://doi.org/10.1515/jmbm-2020-0013
Received Jun 27, 2020; accepted Oct 06, 2020

Abstract: An exact linear elastic solution is derived for a pair of opposing point loads, which act in the middle of a straight slot having rounded ends. This problem is analogous to the mode III crack problem where two concentrated forces act in opposite directions to open the surfaces of a finite-length crack. The corresponding path independent *J* integral for this slot problem is also determined.

Keywords: mode III stress function in curvilinear coordinates, elliptical hole, Riabouchinsky free streamline problem

1 Introduction

Prior to this analysis, no exact solution has been found for a linear slot with rounded ends subject to two opposing antiplane point loads. Perhaps the closest analogy that one may find in the literature is for two opposing point loads acting on the surface of an elliptical hole [1]. However, experience has shown that for remotely applied shear tractions, large differences exist in stress concentration factors for solutions of a slot having this particular geometry and those of an ellipse with identical aspect ratio of slot length to slot width [2, 3]. This observation suggests that it is questionable in general to use the solution of an elliptical hole problem as a close approximation of a solution for a slot.

The shape of the slot analyzed here comes from the free-streamline problem of an ideal fluid flowing past two side-by-side flat plates [4] where the flow at infinity is perpendicular to the plates. The analogy between this solution and that of an antiplane slot problem with a uniform shear loading at infinity was explored in detail in [5, 6]. Further, linear elastic solutions in the plane for remotely applied tensile loadings of a slot of a similar shape was investigated in [7, 8] using numerical methods of analysis.

***Corresponding Author: David J. Unger:** Department of Mechanical and Civil Engineering, University of Evansville, Evansville, IN 47722, United States of America; Email: du2@evansville.edu

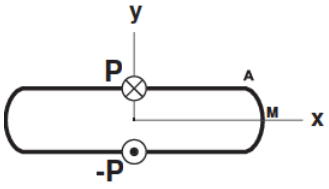

Figure 1: Slot boundary and loads

The mapping function of the plane exterior to the slot of Figure 1 onto a unit circle [5–8] has the form

$$z = \omega(\zeta) = \frac{a}{2}\left\{-(1-k')\frac{1+\zeta^2}{2\zeta} + sgn(\mathrm{Re}\zeta)\left[k'K(m) - E(m)\right] + i(1+k')\left[E\left(\sin^{-1}\frac{i}{k_1}\frac{1-\zeta^2}{2\zeta}, {k_1}^2\right) - \frac{(1-k')^2}{(1+k')^2}F\left(\sin^{-1}\frac{i}{k_1}\frac{1-\zeta^2}{2\zeta}, {k_1}^2\right)\right]\right\}, \quad (1)$$

where a is a scaling factor with units of length and z is the complex variable

$$z = x + iy. \quad (2)$$

In (2), the real and imaginary parts of z represent the Cartesian plane (x, y). The mapping variable of (1) ζ is expressed in polar coordinates by

$$\zeta = \rho\exp(i\theta), \quad 0 \le \rho \le 1, \quad -\pi \le \theta \le \pi, \quad (3)$$

where ρ is the radius, and θ is the angle on and within the unit circle γ. Various relationships among parameters appearing in the elliptic integrals [9] of (1) are

$$m = 1 - m_1, k' = \sqrt{m_1}, \quad k_1 = \frac{2\sqrt{k'}}{1+k'}, \quad 0 \le m_1 \le 1. \quad (4)$$

On the unit circle γ, the parameters of (4) are related to the angle θ by the following relationships

$$k' = \frac{1-\cos\theta_0}{1+\cos\theta_0}, \quad k_1 = \sin\theta_0, \quad (5)$$

where $\pm\theta_0$ and $\pm\pi \mp \theta_0$ are the four locations on the slot boundary ($\rho = 1$) where the flat surfaces meet the rounded surfaces. In Figure 1, point A marks one these locations in the first quadrant of the xy plane.

2 Stress analysis in cartesian coordinates

In the complex plane, a Westergaard stress function [10] is often used to solve mode III crack problems, which are a class of antiplane linear elastic problems for isotropic materials. Accordingly, the Westergaard stress function and its related functions have the following relationships

$$\tau_x = \mathrm{Im} Z_{III} = \frac{\partial \varphi}{\partial y} = G\frac{\partial \delta}{\partial x}, \qquad \tau_y = \mathrm{Re} Z_{III} = -\frac{\partial \varphi}{\partial x} = G\frac{\partial \delta}{\partial y}, \tag{6}$$

where $\tau_x(x, y)$ and $\tau_y(x, y)$ are antiplane shear stresses, $\varphi(x, y)$ is a real-valued stress function, and $\delta(x, y)$ is a real-valued out-of-plane displacement. In (6), the parameter G is the shear modulus, which is assumed constant. The stresses (6) are the only stresses present in this class of problems. Similarly, $\delta(x, y)$ is the only component of displacement in an antiplane problem, which acts in a direction perpendicular to the xy plane.

Now equilibrium requires [10]

$$\frac{\partial \tau_x}{\partial x} + \frac{\partial \tau_y}{\partial y} = 0 \tag{7}$$

which is automatically satisfied by the stress function $\varphi(x, y)$. The compatibility equation for strain further requires [10]

$$\frac{\partial \gamma_x}{\partial y} - \frac{\partial \gamma_y}{\partial x} = 0, \tag{8}$$

where γ_x and γ_y are the engineering shear strains in the x and y directions respectively. As the shear strains are related to the displacement as follows

$$\gamma_x = \frac{\partial \delta}{\partial x}, \quad \gamma_y = \frac{\partial \delta}{\partial y}, \tag{9}$$

the compatibility equations (8) are automatically satisfied by the displacement $\delta(x, y)$.

However, Hooke's law imposes the following additional relationships between stress and strain

$$\tau_x = G\gamma_x, \quad \tau_y = G\gamma_y. \tag{10}$$

Consequently, by substituting (9) into (10) and the resultant stress field into (7), one determines that $\delta(x, y)$ must also satisfy Laplace's equation

$$\frac{\partial^2 \delta}{\partial x^2} + \frac{\partial^2 \delta}{\partial y^2} = 0 \tag{11}$$

for equilibrium to be satisfied.

Similarly, by substituting the relationships for the shear stresses involving partial derivatives of φ from (6) into (10) to obtain their relationships with strain, one concludes by substituting these strains into (8) that φ must also satisfy Laplace's equation in order that the strain compatibility equation be satisfied

$$\frac{\partial^2 \varphi}{\partial x^2} + \frac{\partial^2 \varphi}{\partial y^2} = 0. \tag{12}$$

Therefore, as relationships (6) indicate, φ and $G\delta$ are conjugate harmonic functions. Consequently, their relationships are consistent with the general properties of the real and imaginary parts of a complex function of z [11], which in this case is the Westergaard stress function.

3 Stress analysis in curvilinear coordinates

Often, the solution of a problem with complicated boundaries can be simplified by the adoption of an appropriate orthogonal curvilinear coordinate system that accommodates the boundaries naturally. Let us suppose that it is useful to define such a system as follows

$$z = f(w), \quad w = u + iv, \tag{13}$$

where f is an arbitrary function and u and v are real functions that constitute an orthogonal curvilinear coordinate system by virtue of the properties of a function of a complex variable [11].

It is the goal here to develop a connection between the curvilinear coordinate system defined by (13) and the previously defined functions of (6). Using the chain rule of partial differentiation, one finds that for the stress function φ

$$\frac{\partial \varphi}{\partial x} = \frac{\partial \varphi}{\partial u}\frac{\partial u}{\partial x} + \frac{\partial \varphi}{\partial v}\frac{\partial v}{\partial x}, \qquad \frac{\partial \varphi}{\partial y} = \frac{\partial \varphi}{\partial u}\frac{\partial u}{\partial y} + \frac{\partial \varphi}{\partial v}\frac{\partial v}{\partial y}. \tag{14}$$

It is now useful to interchange what are the dependent and independent variables in the partial derivatives of the coordinates in (14) as follows [12]

$$\frac{\partial u}{\partial x} = \frac{1}{\Delta}\frac{\partial y}{\partial v}, \quad \frac{\partial v}{\partial x} = -\frac{1}{\Delta}\frac{\partial y}{\partial u}, \quad \frac{\partial u}{\partial y} = -\frac{1}{\Delta}\frac{\partial x}{\partial v}, \quad \frac{\partial v}{\partial y} = \frac{1}{\Delta}\frac{\partial x}{\partial u}, \tag{15}$$

$$\text{where } \Delta = \frac{\partial x}{\partial u}\frac{\partial y}{\partial v} - \frac{\partial y}{\partial u}\frac{\partial x}{\partial v}.$$

Certain geometric relationships exist between the antiplane shear stresses in the (u, v) directions respectively τ_u and τ_v and their Cartesian counterparts. By resolution of the in-plane stress vectors, one finds

$$\tau_u = \tau_x \cos\alpha + \tau_y \sin\alpha \tag{16}$$

$$\tau_v = -\tau_x \sin\alpha + \tau_y \cos\alpha,$$

where α is the angle between the x axis and the direction of a unit vector in the u direction.

By substituting (15) into (14) and using the definitions of τ_x and τ_y and in terms of the stress function φ of (6), one can derive from these relationships and (16) that

$$\tau_u = \frac{\left(\frac{\partial x}{\partial v}\cos\alpha + \frac{\partial y}{\partial v}\sin\alpha\right)\frac{\partial \varphi}{\partial u} - \left(\frac{\partial x}{\partial u}\cos\alpha + \frac{\partial y}{\partial u}\sin\alpha\right)\frac{\partial \varphi}{\partial v}}{\frac{\partial x}{\partial v}\frac{\partial y}{\partial u} - \frac{\partial x}{\partial u}\frac{\partial y}{\partial v}}, \tag{17}$$

$$\tau_v = \frac{\left(\frac{\partial y}{\partial v}\cos\alpha - \frac{\partial x}{\partial v}\sin\alpha\right)\frac{\partial \varphi}{\partial u} + \left(\frac{\partial x}{\partial u}\sin\alpha - \frac{\partial y}{\partial u}\cos\alpha\right)\frac{\partial \varphi}{\partial v}}{\frac{\partial x}{\partial v}\frac{\partial y}{\partial u} - \frac{\partial x}{\partial u}\frac{\partial y}{\partial v}}. \tag{18}$$

At this point it is helpful to introduce the metric coefficient

$$h = \left|\frac{dz}{dw}\right|. \tag{19}$$

Using relationships similar to those derived in [13]

$$\frac{\partial x}{\partial u} = h\cos\alpha, \quad \frac{\partial y}{\partial u} = h\sin\alpha, \qquad \frac{\partial x}{\partial v} = -h\sin\alpha, \quad \frac{\partial y}{\partial v} = h\cos\alpha, \tag{20}$$

one finds the denominator of relationships (17) and (18) as

$$\frac{\partial x}{\partial v}\frac{\partial y}{\partial u} - \frac{\partial x}{\partial u}\frac{\partial y}{\partial v} = -h^2. \tag{21}$$

Upon substitution of (20) and (21) into (17) and (18), there is a reduction of these expressions to the following simple forms

$$\tau_u = \frac{1}{h}\frac{\partial \varphi}{\partial v}, \quad \tau_v = -\frac{1}{h}\frac{\partial \varphi}{\partial u}. \tag{22}$$

Because of (12), the function φ must also satisfy Laplace's equation, which in the (u, v) system assumes the form

$$\frac{\partial^2 \varphi}{\partial u^2} + \frac{\partial^2 \varphi}{\partial v^2} = 0. \tag{23}$$

4 Elliptical hole analysis

In order to gain insight into the slot solution, let us first explore the solution of the analogous elliptical hole point load problem, which has a known solution [1]. The mapping function of the boundary of an elliptical hole in an infinite plate onto the surface and interior of a unit circle has the form [15]

$$z = \omega(\zeta) = R\left(M\zeta + 1/\zeta\right), \tag{24}$$

where

$$R = \frac{a+b}{2}, \quad M = \frac{a-b}{a+b}. \tag{25}$$

In (25), a is the semimajor axis and b is the semiminor axis of the ellipse. The mapping function of the elliptical hole on the unit circle will have the same form as (3) for the associated polar coordinates.

Let us now define the following function, which has logarithmic singularities at $\zeta = \pm i$,

$$\varphi_C(\zeta) = A\tan^{-1}\zeta, \tag{26}$$

where A is a parameter to be determine from equilibrium in terms of the point loads P. By differentiation of (26) with respect to ζ, one finds that the function has $1/r$ singularities at $\zeta = \pm i$. These properties characterize stresses that are typically associated with point loads in linear elasticity theory. The derivative of (26) with respect to ζ is explicitly

$$\varphi'_C(\zeta) = \frac{A}{1+\zeta^2}. \tag{27}$$

Now assume a Westergaard stress function of the form

$$Z_{III} = \frac{d\varphi_C}{dz}, \tag{28}$$

which has the following alternative representation in terms of ζ using the chain rule of differential calculus

$$Z_{III}(\zeta) = \frac{\varphi'_C(\zeta)}{\omega'(\zeta)}, \tag{29}$$

where $\omega'(\zeta)$ is the first derivative of (24) with respect to ζ,

$$\omega'(\zeta) = R\left(M - 1/\zeta^2\right). \tag{30}$$

Upon substitution of (25), (27), and (30) into (29), the Westergaard stress function becomes

$$Z_{III}(\zeta) = \frac{2A\zeta^2}{\left(1+\zeta^2\right)\left[(a-b)\zeta^2 - (a+b)\right]}. \tag{31}$$

Now to determine the constant A of (31) one needs to evaluate the integral appearing in the following expression

$$\frac{1}{2}|P| = \left|\int_a^\infty \tau_y|_{y=0}\, dx|_{y=0}\right|. \tag{32}$$

This relationship reflects a symmetry requirement that one half of the magnitude of the load P must be carried along the positive x axis from the tip of the semimajor axis to infinity. In terms of the coordinates defined by (3), the relationships to the right of the integral sign of (32) are

$$dx|_{y=0} = \frac{a\left(\rho^2 - 1\right) - b\left(\rho^2 + 1\right)}{2\rho^2}\, d\rho, \tag{33}$$

$$\tau_y|_{y=0} = \frac{2A\rho^2}{(\rho^2+1)\left[a\left(\rho^2-1\right)-b\left(\rho^2+1\right)\right]}.$$

The evaluation of (32) with the substitutions (33) indicate

$$\frac{1}{2}|P| = \left|A\int_1^0 \frac{d\rho}{1+\rho^2}\right| \rightarrow A = \mp\frac{2}{\pi}P, \tag{34}$$

where the sign in (34) is determined by the directions of the loads.

Let us now introduce cylindrical elliptical coordinates (u, v) in terms of complex variable notation as follows

$$z = c\cosh w \text{ where } w = u + iv, \tag{35}$$
$$\text{for} \quad 0 \le u \le \infty, \quad -\pi \le v \le \pi,$$

where $2c$ is the distance on the x axis between the foci of the ellipses. Correspondingly, in the real plane [14] from (2) and (35)

$$x = c\cosh u\cos v, \quad y = c\sinh u\sin v. \tag{36}$$

The equation of equilibrium in cylindrical elliptical coordinates for the antiplane problem is derived from a more general relationship given in [15] as

$$\frac{\partial}{\partial u}(h\tau_u) + \frac{\partial}{\partial v}(h\tau_v) = 0. \tag{37}$$

The specific form of the metric coefficient h for (37) is determined from (19) and (35) to be [14]

$$h = c\sqrt{\frac{\cosh 2u - \cos 2v}{2}} \tag{38}$$
$$= c\sqrt{\sinh^2 u + \sin^2 v}.$$

Note that relationships (22) automatically satisfy (37); however, φ must additionally solve Laplace's equation (23) in order to ensure the compatibility of strains.

Now by introducing elliptical coordinates into (26), one finds by taking the real part [9] of (26) that

$$\varphi = \mathrm{Re}\varphi_C(\zeta) = \mathrm{Re}\varphi_C\left(e^{u_0 - w}\right), \tag{39}$$
$$= \frac{A}{2}\tan^{-1}\left(\frac{\cos v}{\sinh(u-u_0)}\right),$$

where u_0 is the value of the coordinate u of the elliptical hole.

By direct substitution, it is easy to verify that (39) satisfies Laplace's equation (23). It also follows from (36) that

$$a = c\cosh u_0, \quad b = c\sinh u_0. \tag{40}$$

From (22), (38), and (39), one obtains the solution for the stresses as

$$\tau_u = \pm\frac{2P}{\pi h}\frac{\sinh(u-u_0)\sin v}{\cosh 2(u-u_0)+\cos 2v}, \tag{41}$$

$$\tau_v = \mp\frac{2P}{\pi h}\frac{\cosh(u-u_0)\cos v}{\cosh 2(u-u_0)+\cos 2v},$$

where h in (41) is given by (38). The upper signs of (41) correspond to $A = -2P/\pi$, which agree with the loading directions shown in Figure 1 for the analogous slot problem.

A plot of the stress function φ is shown in Figure 2 for $c = 1$, $u_0 = 0.2$, and $P = 1$. Note that the stress function is constant along the elliptical hole u_0 except for a jump that occurs at $v = \pm\pi/2$, where the point loads are applied.

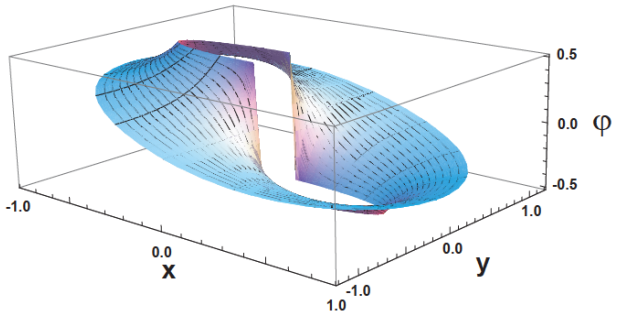

Figure 2: Stress function for elliptical hole

On the elliptical hole $u = u_0$, one determines from (41) that the boundary condition on traction is satisfied as τ_u is everywhere zero except at the locations of the concentrated loads, which are singularities. This behavior is depicted in Figure 3.

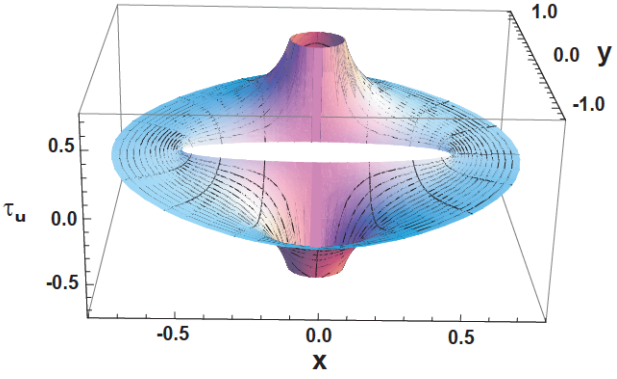

Figure 3: Shear stress for elliptical hole in the u-direction

A local maximum value of the shear stress, away from the point loads, is consistent with the value determined previously in [1]

$$\left|\tau_{\max}^{\text{local}}\right| = |\tau_v(u_0, 0)| = \frac{P}{\pi b}, \tag{42}$$

which occur at the ends of the major axes as shown in Figure 4. In general, Figure 4 illustrates the behavior of the τ_v stress field near the slot.

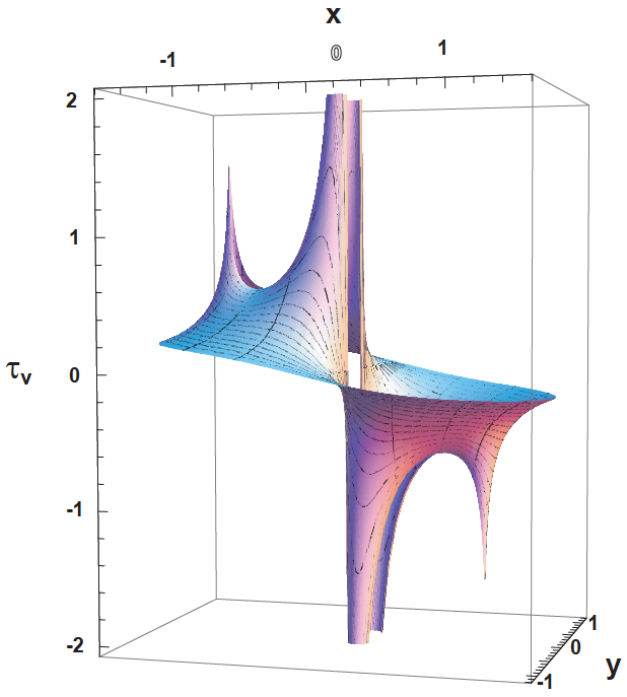

Figure 4: Shear stress for elliptical hole in the v-direction

It should be mentioned that cylindrical elliptical coordinates were not employed in the solution presented in [1], nor were explicit forms of the stresses provided as in (41).

5 Slot analysis

Now that experience has been gained by working through the simpler elliptical hole problem, the analogous slot solution of Figure 1 will be derived.

By taking the first derivative of (1) with respect to ζ, one finds

$$\omega'(\zeta) = \frac{a}{4}\left(1-k'\right)\frac{1-\zeta^2}{\zeta^2} + \operatorname{sgn}(\operatorname{Re}\zeta) \times \frac{a\sqrt{k'}}{\zeta}\sqrt{1+\frac{1}{k_1^2}\left(\frac{1-\zeta^2}{2\zeta}\right)^2} \tag{43}$$

The functions analogous to those of (26)–(29) assume similar forms to those given previously for the elliptical hole. They provide upon substitution of (43) for $\omega'(\zeta)$ in (29) the following form of the Westergaard function for the slot

$$Z_{III} = \frac{2A\zeta^2(1+\cos\theta_0)}{a\left(1+\zeta^2\right)\left[\cos\theta_0\left(1-\zeta^2\right)+g(\zeta)\right]}, \tag{44}$$

where

$$g(\zeta) = sgn(\operatorname{Re}\zeta)\,\zeta\sqrt{\zeta^2 - 2\cos 2\theta_0 + \zeta^{-2}}.$$

The relationship between A and P is determined for the slot problem from equilibrium considerations in much the same way as for the elliptical hole. However, direct integration of the expressions involved are much more complicated than they were for the elliptical hole. See Appendix A for details of the evaluation of the integral indirectly. The result of this integration is identical to the value of A found previously for the elliptical hole in terms of the concentrated load P for the directions shown in Figure 1,

$$A = -\frac{2P}{\pi}. \tag{45}$$

Next, a coordinate system resembling cylindrical elliptical coordinates will be introduced for the slot problem by substituting for ζ in (1) the following relationship [8]

$$\zeta = -\exp(-w), \quad w = u + iv, \quad 0 \le u \le \infty, \quad -\pi \le v \le \pi. \tag{46}$$

Along the slot surface $u = 0$ in this coordinate system. Now the real-valued stress function assumes the following form for the slot problem in these coordinates

$$\varphi = -\frac{P}{\pi}\tan^{-1}\left(\frac{\cos v}{\sinh u}\right). \tag{47}$$

The shape of the stress function (47) is shown in Figure 5. By substituting (46) into (43) the metric coefficient h is determined to be

$$h = \sqrt{\operatorname{Re}(dz/dw)^2 + \operatorname{Im}(dz/dw)^2}, \tag{48}$$

where

$$\operatorname{Re}(dz/dw) = \frac{a}{2}\left(1-k'\right)\sinh u\cos v + a\sqrt{\frac{k'}{2}}\operatorname{sgn}(\pi/2-|v|)\sqrt{a_1+\sqrt{a_1^2+b_1^2}} \tag{49}$$

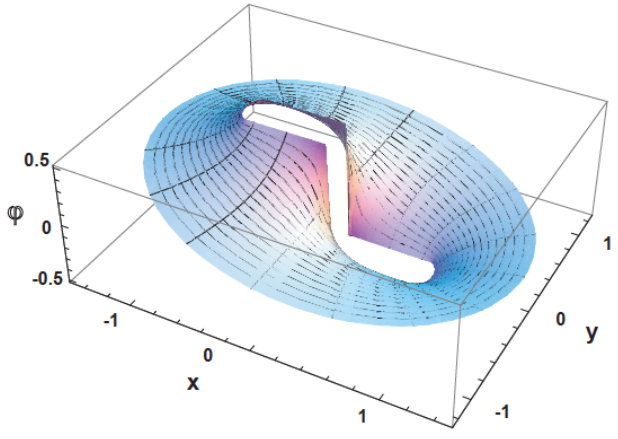

Figure 5: Stress function for the slot

$$\mathrm{Im}\,(dz/dw) = \frac{a}{2}\,(1-k')\cosh u \sin v + \mathrm{sgn} b_1 \times a\sqrt{\frac{k'}{2}}\,\mathrm{sgn}\,(\pi/2-|v|)\,\sqrt{-a_1+\sqrt{a_1^2+b_1^2}} \tag{50}$$

with

$$a_1 = 1 + \frac{\sinh^2 u\cos^2 v - \cosh^2 u \sin^2 v}{k_1^2}, \tag{51}$$
$$b_1 = \frac{2\cosh u \sinh u \cos v \sin v}{k_1^2}.$$

The shear stresses follow from (22) as

$$\tau_u = \frac{2P}{\pi h}\frac{\sinh u \sin v}{\cosh 2u + \cos 2v}, \tag{52}$$
$$\tau_v = -\frac{2P}{\pi h}\frac{\cosh u \cos v}{\cosh 2u + \cos 2v},$$
$$0 \le u \le \infty, -\pi \le v \le \pi,$$

where h is given by (48). These stresses are plotted in Figures 6 and 7 respectively for value of $m_1 = 0.01$, $a = 1$, and $P = 1$.

The value of a local maximum of the shear stress, away from the point loads, is found at the four locations where the flat surfaces of the slot meet the rounded ends of the slot along its boundary. This value at point A of Figure 1 is

$$\left|\tau_{\max}^{\mathrm{local}}\right| = |\tau_v(0,\theta_0)| = |\tau_A| = \frac{P}{\pi a\, m_1^{1/4}}\left(\frac{1+m_1}{1-m_1}\right)^2. \tag{53}$$

At the extreme ends of the slot, as represented by point M of Figure 1, the magnitude of the shear stress τ_v is lower than that of point A of Figure 1

$$|\tau_M| = \frac{P}{\pi a\, m_1^{1/4}}. \tag{54}$$

The location where the maximum stress occurs in a slot of this geometry can differ in how the load is applied. For example, in the case of uniform tensile loadings at infinity, the largest principal stress occurs at a point analogous to point M of Figure 1, provided the direction of the applied load is perpendicular to the long axis of the slot [8]. Similarly, in the case of uniform biaxial tensile loadings of the slot at infinity, the maximum value of the principal stress falls somewhere between points M and A of Figure 1 along the curved portion of the slot depending on the value of m_1.

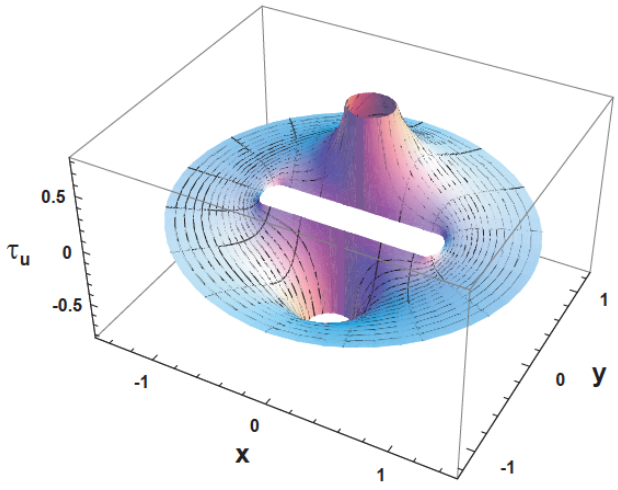

Figure 6: Shear stress for the slot in the u-direction

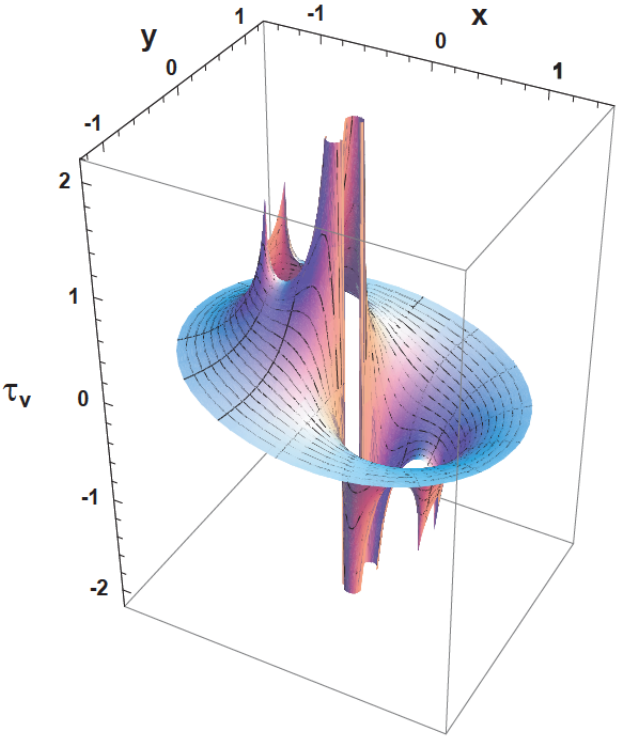

Figure 7: Shear stress for the slot in the v-direction

6 Path independent integral for slot problem

The path-independent J integral has shown to be a useful tool in the analysis of crack growth problems. The geometry of the slot of Figure 1 can serve as a crack having a finite width with rounded tips. The J integral as defined in [16] reduces to the following form for this problem

$$J = \int_{\Gamma} W dy, \tag{55}$$

where W is the strain energy density and Γ is the path of integration. The J integral for this particular slot problem can be reduced to the evaluation of this integral along a path limited to the rounded portion of the left hand side of

the slot. This evaluation will be performed using the coordinate θ of (3). In [5], the angle θ was related to a conformal mapping of the region exterior to the slot onto the surface and interior of a unit circle. The positive direction for the angle θ on the unit circle is in the counterclockwise direction. In the physical plane, the angle $\theta = 0$ defines a ray that begins at the origin of the xy coordinate system and continues along the negative x axis. A point on the surface of the slot traverses a path in the clockwise direction for a change of the angle θ in the counterclockwise direction.

The form of W for the antiplane problem addressed here is

$$W = \frac{1}{2G}\left(\tau_x^2 + \tau_y^2\right) = \frac{1}{2G}\left(\mathrm{Re}Z_{III}^2 + \mathrm{Im}Z_{III}^2\right). \tag{56}$$

The following expressions are obtained along the surface of the slot from (44) where ρ of (3) is set equal to one

$$\mathrm{Re}Z_{III} = \frac{P\left(1+\cos\theta_0\right)\csc^2\theta_0 \sec^3\theta\sqrt{\cos 2\theta - \cos 2\theta_0}}{\sqrt{2}\pi a}, \quad -\theta_0 \le \theta \le \theta_0. \tag{57}$$

$$\mathrm{Im}Z_{III} = \frac{P\left(1+\cos\theta_0\right)\cot\theta_0 \csc\theta_0 \sec^2\theta\tan\theta}{\pi a}, \quad -\theta_0 \le \theta \le \theta_0. \tag{58}$$

With (57) and (58) the form of (56) reduces to

$$W = \frac{P^2\cot^2\left(\theta_0/2\right)\sec^4\theta}{2\pi^2 a^2 G}, \quad -\theta_0 \le \theta \le \theta_0. \tag{59}$$

Along the rounded portion of the of the left hand slot tip

$$y = \frac{a}{1+\cos\theta_0}\left[E\left(\sin^{-1}\left(\sin\theta/\sin\theta_0\right), \sin^2\theta_0\right) - \cos^2\theta_0 F\left(\sin^{-1}\left(\sin\theta/\sin\theta_0\right), \sin^2\theta_0\right)\right], \tag{60}$$

for $-\theta_0 \le \theta \le \theta_0$.

Taking the derivative of y of (60) with respect to θ gives

$$\frac{dy}{d\theta} = \frac{a\left(\cos 2\theta - \cos 2\theta_0\right)\csc\theta_0}{2(1+\cos 2\theta_0)\sqrt{1-\left(\sin\theta/\sin\theta_0\right)^2}}. \tag{61}$$

Now, using properties of trigonometric functions, one can show

$$\cos 2\theta - \cos 2\theta_0 = \left(1-\cos 2\theta_0\right)\left[1-\left(\sin\theta/\sin\theta_0\right)^2\right]. \tag{62}$$

Consequently, when (59), (61), and (62) are substituted into (55), one obtains after use of some trigonometric identities

$$J = \frac{P^2\cot\left(\theta_0/2\right)}{2\pi^2 aG}\int_{-\theta_0}^{\theta_0}\sqrt{1-\left(\sin\theta/\sin\theta_0\right)^2}\sec^4\theta d\theta. \tag{63}$$

For the purposes of evaluation, this integral is further simplified by making the following substitutions into it

$$s = \sin\theta/\sin\theta_0 \rightarrow d\theta = \frac{\sin\theta_0\, ds}{\sqrt{1-\sin^2\theta_0\, s^2}}, \tag{64}$$

to generate

$$J = \frac{2P^2\cos^2\left(\theta_0/2\right)}{\pi^2 aG}\int_0^1 \frac{\sqrt{1-s^2}\, ds}{\left(1-\sin^2\theta_0\, s^2\right)^{5/2}}, \tag{65}$$

where the factor of two before the integral results from the symmetry of the integrand and an adjustment of the limits of integration. The integral in (65) is readily evaluated using the symbolic computer program Mathematica® as

$$J = \frac{2P^2\cos^2\left(\theta_0/2\right)}{3\pi^2 aG}\left[\csc^2\theta_0\, K\left(\sin^2\theta_0\right) - 4\cot\left(2\theta_0\right)\csc\left(2\theta_0\right)E\left(\sin^2\theta_0\right)\right]. \tag{66}$$

The limit of J as $\theta_0 \rightarrow 0$ corresponds to the value of a mode III crack subject to a pair of antiplane splitting forces applied at the middle of the crack

$$J_0 = \lim_{\theta_0\rightarrow 0} J = \frac{P^2}{2\pi aG}. \tag{67}$$

This is consistent with the value determined by substituting the stress intensity factor K_{III} for a pair of opposed point loads P applied at the middle of a line crack of length $2a$ [17], *i.e.*,

$$K_{III} = \frac{P}{\sqrt{\pi a}}, \tag{68}$$

into a general relationship for the J integral [18] for mode III crack problems

$$J_{III} = \frac{K_{III}^2}{2G} \tag{69}$$

The range of J/J_0 varies monotonically from a value of one for $\theta_0 = 0$ to infinity for $\theta_0 = \pi/2$.

7 Closing

A prototype problem for the loading of a slot by forces applied near the center of its internal boundary was proposed and solved in this article The singularities that appear at the points of application of the concentrated loads

were anticipated and consequently they are not particularly noteworthy. However, of considerable interest is how this symmetrical loading near the center of a slot generates states of stress at other locations along the slot boundary. For example, it was not known beforehand if the applied loads would generate larger states of stress at points A or M of Figure 1.

One notes that the linear elastic point load problem presented here is only the second analytical solution known for a slot with rounded ends. The first [2, 3, 5, 6] was found by analogy with the free streamline problem of Riabouchinsky [4]. That particular slot solution assumes a load of uniform antiplane shear tractions at infinity rather than point loads applied along its interior boundary. In both cases, however, one finds large stresses that are proportional to $1/m_1^{1/4}$ at the slot tips. Consequently, as the geometry of the slot approaches that of a line crack ($m_1 \to 0$), the stresses at the tips become singular in a similar mathematical fashion with m_1 for the two different types of loading.

Further, the J integral for the slot was found here in a straightforward manner that is impossible to duplicate with the analogous loading of an elliptical hole. If one attempts to calculate the J integral along the periphery of an elliptical hole, one encounters a divergent integral because of the presence of the singularities generated by the point loads. This issue is not encountered in the slot problem because the path of integration is limited to the rounded portions of the slot. Along the flat surfaces of the slot, where the point loads are applied, dy is zero, which negates the effect of the singularities on the convergence of the integral. In a similar light, the calculation of the J integral for the line crack cannot be determined by following a path along the surfaces of the crack as dy equals zero along them and there is no smooth curve connecting the surfaces. Nevertheless, one may determine the value of the J integral for the line crack (67) subject to opposing point loads from the solution for the slot (66). One simply allows the parameter m_1 to approach zero, which causes the flat surfaces of the slot to converge to a line crack of length $2a$ with zero width.

References

[1] Neuber H. Kerbspannungslehre. 4th ed. Berlin: Springer; 2001:36.

[2] Unger DJ. Linear elastic solutions for slotted plates. J Elast. 2012;108(1):67-82.

[3] Unger DJ. Erratum to: linear elastic solutions for slotted plates. J Elast. 2012;108(1):83.

[4] Riabouchinsky D., On steady fluid motions with free surfaces, Proc. Lond. Math. Soc. (2) 1921;19(1):206-215

[5] Unger DJ. Free streamline hydrodynamic analogy for a linear elastic antiplane slot problem with perfectly plastic ligaments at its ends. J Elast. 2018;132(2):261-70.

[6] Unger DJ. Visualizing the crack driving force through fluid analogy. J Mech Behav Mater. 2019;28(1):89-94.

[7] Unger DJ. Linear elastic solutions for slotted plates revisited, Proceedings 24th International Congress of Theoretical and Applied Mechanics, ed. JM Floryan, ICTAM, Montreal; 2017:2042-2043.

[8] Unger DJ. Comparison of series and finite difference solutions to remote tensile loadings of a plate having a linear slot with rounded ends. J Mech Mater Struct. 2020;15(3):361-78.

[9] Abramowitz M, Stegun IA. Handbook of Mathematical Functions with Formulas, Graphs and Mathematical Tables. National Bureau of Standards, Series 55, U.S. Printing Office, Washington, DC, 1964; 81:589-628.

[10] Unger DJ. Analytical Fracture Mechanics. Dover: Mineola; 2011:29-34.

[11] Churchill RV. Complex Variables and Applications. New York: McGraw-Hill. 1960.

[12] Kachanov LM. Fundamentals of the Theory of Plasticity. Dover: Mineola; 2004:469-70.

[13] Timoshenko SP, Goodier JN. Theory of Elasticity. 3rd ed. New York: McGraw-Hill; 1934:184.

[14] Spiegel MR, Liu J. Mathematical Handbook of Formulas and Tables, 2nd ed., Shaum's Outline, McGraw-Hill, New York; 1999:127.

[15] Sokolnikoff IS. Mathematical Theory of Elasticity, 2nd ed., McGraw-Hill, New York; 1956;181:292.

[16] Rice JR. A path independent integral and approximate analysis of strain concentrations by notches and cracks. J Appl Mech. 1968;35(2):379-86.

[17] Tada H, Paris PC, Irwin GR. The Stress Analysis of Cracks Handbook. 3rd ed. New York: ASME; 2000, 138.

[18] Broberg KB. Cracks and Fracture. San Diego: Academic Press; 1999, 77

Appendix A

Evaluation of parameter A

In this appendix, the parameter A of (27) will be evaluated from equilibrium considerations for the slot problem.

One notes the following differential relationship from (1) and (29)

$$Z_{III}dz = \frac{\varphi'_C(\zeta)}{\omega'(\zeta)}\omega'(\zeta)\,d\zeta. \tag{A1}$$

Upon integrating both sides of (A1), one finds between limits of integration

$$\int_{z_1}^{z_2} Z_{III}(z)dz = \int_{\zeta_1}^{\zeta_2} \varphi'_C(\zeta)d\zeta = \varphi_C(\zeta_2) - \varphi_C(\zeta_1). \tag{A2}$$

By substituting the following expressions into (A2) and expanding

$$\begin{aligned} Z_{III} &= \mathrm{Re}Z_{III} + i\mathrm{Im}Z_{III}, \\ dz &= dx + idy, \end{aligned} \tag{A3}$$

one obtains

$$\begin{aligned} \int_{z_1}^{z_2} Z_{III}(z)dz = &\int_{x_1}^{x_2} \mathrm{Re}Z_{III}dx - \int_{y_1}^{y_2} \mathrm{Im}Z_{III}dy \\ &+ i\int_{y_1}^{y_2} \mathrm{Re}Z_{III}dy + i\int_{x_1}^{x_2} \mathrm{Im}Z_{III}dx \end{aligned} \tag{A4}$$

Now restricting attention to the positive x axis, one may set both $dy = 0$ and $\mathrm{Im}Z_{III}$ equal to zero in (A4). The latter is valid because it is equal to τ_x, which produces no traction along the x axis in the y direction. What remains of (A4) reflects the load that must be carried along the right hand side of the plane. For the direction of loading shown in Figure 1, one has

$$\int_{x_1}^{x_2} \mathrm{Re}Z_{III}dx = \int_{x_M}^{\infty} \tau_y dx = -\frac{P}{2}. \tag{A5}$$

Further, the right hand side of (A2) becomes by substituting φ_C from (26) into it

$$\varphi_C(\zeta_2) - \varphi_C(\zeta_1) = A\tan^{-1}\zeta_2 - A\tan^{-1}\zeta_1, \tag{A6}$$

Now, for the right hand side of (A6), a change of variables is introduced using (46)

$$A\tan^{-1}\exp(-w_1) - A\tan^{-1}\exp(-w_2). \tag{A7}$$

The complex variables w_1 and w_2 found in (A7) are defined in terms of the real-valued coordinates (u, v) by

$$w_1 = u_1 + iv_1, \quad w_2 = u_2 + iv_2, \tag{A8}$$

By substituting w_1 and w_2 from (A8) into (A7) and evaluating the expression using the following limits of integration along the positive x axis

$$u_1 = 0, \quad u_2 \to \infty, \quad v_1 = v_2 = 0, \tag{A9}$$

one obtains

$$A\tan^{-1}1 - A\lim_{u_2\to\infty}\tan^{-1}e^{-u_2} = A\,\pi/4. \tag{A10}$$

Consequently, equating the right hand side of (A5) to the right hand side of (A10) quantifies the value of A in terms of P as

$$-\frac{P}{2} = A\frac{\pi}{4} \to A = -\frac{2P}{\pi}. \tag{A11}$$